Arch. Min. Sci. **66** (2021), 3, 475-490

Electronic version (in color) of this paper is available: http://mining.archives.pl

DOI 10.24425/ams.2021.138601

XIAO QU[1*], SHAOJIE CHEN[2], DAWEI YIN[2], SHIQI LIU[1]

EXPERIMENTAL STUDY OF THE STRIP COAL PILLAR MODELS FAILURE WITH DIFFERENT ROOF AND FLOOR CONDITIONS

In order to study the failure mechanism and characteristics for strip coal pillars, a monitoring device for strip coal pillar uniaxial compression testing was developed. Compression tests of simulated strip coal pillars with different roof and floor rock types were conducted. Test results show that, with increasing roof and floor strength, compressive strength and elastic modulus of "roof-strip coal pillar-floor" combined specimens increase gradually. Strip coal pillar sample destruction occurs gradually from edge to the interior. First macroscopic failure occurs at the edge of the middle upper portion of the specimen, and then develops towards the corner. Energy accumulation and release cause discontinuous damage in the heterogeneous coal-mass, and the lateral displacement of strip coal pillar shows step and mutation characters. The brittleness and burst tendency of strip coal pillar under hard surrounding rocks are more obvious, stress growth rate decreases, and the rapid growth acoustic emission (AE) signal period can be regarded as a precursor for instability in the strip coal pillar. The above results have certain theoretical value for understanding the failure law and long-term stability of strip coal pillars.

Keywords: "roof-strip coal pillar-floor" combined specimen, failure characteristics, acoustic emission, laboratory experiment

1. Introduction

Strip mining has become an effective method of coal mining under buildings, railways and water bodies. As a partial mining method, unlike room and pillar mining methods, strip mining can effectively limit overlying strata and surface subsidence as well as protect surface structures. In China, there are thousands of left-over strip coal pillars. With the continued exploitation of

[1] HOHAI UNIVERSITY, CHINA
[2] SHANDONG UNIVERSITY OF SCIENCE AND TECHNOLOGY, CHINA
* Corresponding author: quxiaohhu@163.com

© 2021. The Author(s). This is an open-access article distributed under the terms of the Creative Commons Attribution-NonCommercial License (CC BY-NC 4.0, https://creativecommons.org/licenses/by-nc/4.0/deed.en which permits the use, redistribution of the material in any medium or format, transforming and building upon the material, provided that the article is properly cited, the use is noncommercial, and no modifications or adaptations are made.

coal resources, the number of strip coal pillar is still increasing. These coal pillars are potential hazards for the safe production of coal and development of other industries in the mining area.

In recent years, scholars have examined the design and stability analysis of isolated and protective coal pillars, but few have examined the long-term bearing capacity and failure characteristics of strip coal pillars. Most of the early research on strip coal pillars was based on statistical analysis of a large number of failures of strip coal pillars [1-3]. Khair et al. analyzed geological conditions and the instability collapse characteristics of strip coal pillars and studied the causes and mechanisms of strip coal pillar instability in southern West Virginia [4]. Ghasemi et al. established a prediction model for strip coal pillar stability using logistic regression and fuzzy logic, and predicted the stability of strip coal pillars [5]. Using the 3D laser technology, Kajzar et al. monitored the displacement law of a strip coal pillar within two years aftesr mining in OKD coal mine and studied the long-term stability and creep bearing capacity [6]. Guo et al. studied the stability and overburden displacement of strip coal pillars using the similar materials simulation method and put forward a design method for strip coal pillars used in deep mining [7]. Chen et al. field observed the lateral displacement law of strip coal pillars in deep mining and found that the energy accumulation and release caused a discontinuous damage in the heterogeneous coal-mass. The lateral displacement of strip coal pillars shows discontinuity and mutation characteristics [8].

As part of the "roof-coal-floor" mining system, the stability and failure characteristics of strip coal pillars should be considered in the whole mining system. Roof and floor failure as well as stress changes in the rock-mass can lead to slow or sudden instabilities in strip coal pillars [9-12]. He et al. established the instability mechanical model for the "roof-coal pillar" system, examined the strain-softening properties of coal pillars, and determine the mutation mechanism for coal and overall rock system [13]. Gao et al. proposed a composite rock-mass calculation method based on elastoplastic mechanics and analyzed the influence of the roof and floor on the stability of strip coal pillars [14]. Zuo et al. carried out triaxial compression tests on "coal-rock" combined specimens, and the strength of combined specimen was analyzed using the Hoek-Brown failure criterion [15,16]. Chen et al. carried out uniaxial compression tests on "roof-coal pillar" structures with different width to height ratios, analyzing the mechanical properties and failure mechanisms [17].

At present, numerous studies have examined the design and stability analysis of coal pillars, but few have examined the failure characteristics of large strip coal pillars and the long-term stability of coal-rock systems. In this paper, based on the engineering mechanics model for strip coal pillar, a monitoring device for compression testing strip coal pillars was developed, long-term bearing tests for strip coal pillars with different roof and floor conditions were conducted, and the progressive failure characteristics and mechanical properties of strip coal pillars were analyzed, which is of great significance for understanding the failure characteristics and the stability of strip coal pillars.

2. Mechanical analysis of coal and the rock mass system

2.1. Engineering mechanical model for strip coal pillars

Strip mining means dividing strip area along certain direction in the mining area, the remaining strip coal pillars support the load of overlying strata and are commonly regular cuboid (Fig. 1). After mining, strip coal pillar strain and roof caving are not taken into account, consid-

ering that the interface of strip coal pillar is in complete contact with the roof and floor (Fig. 2). The X-axis is defined as the strike direction of the strip coal pillar, the Y-axis is the inclination direction, and the Z-axis is the vertical direction. On the Z-axis, the overburden pressure and the reaction pressure of floor for the strip coal pillar are simplified into a uniform load. On the X-axis, displacement of the strip coal pillar is constrained. On the Y-axis, the two faces of coal pillar adjacent to the goaf are unrestrained faces.

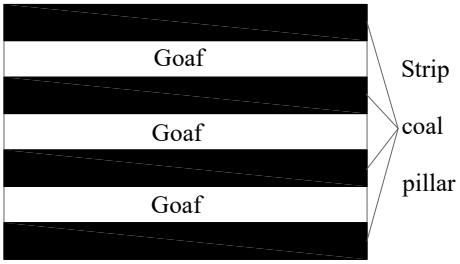

Fig. 1. Layout of strip mining

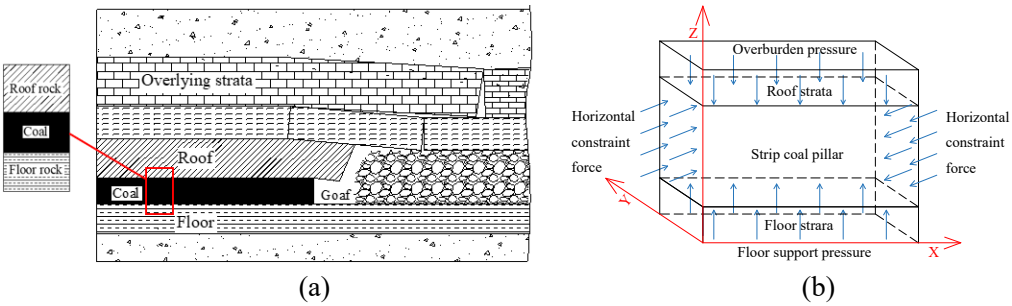

Fig. 2. Schematic diagram of the strip coal pillar mechanical model.
(a) Structures of rock and coal layers; (b) Engineering mechanical model of strip coal pillar

2.2. The effect of friction on coal and rock mass

The friction effect of roof and floor on strip coal pillar according to the plane strain method. The plane strain can be calculated using formula (1) as follows [18]:

$$\varepsilon_x = -\mu(1+\mu) \quad \sigma_y / E \tag{1}$$

where ε_x is the horizontal strain on x-direction; μ is poisson's ratio; E is elastic modulus; σ_y is the normal stress of the overlying strata on y-direction.

A, B, and C are used to represent roof, strip coal pillar and floor respectively, and the elastic modulus and Poisson's ratio of A, B, and C are E_A, E_B, E_C, μ_A, μ_B, μ_C. The interface between the coal and rock is continuous, and the strain in the coal and rock at the interface is equal. According to the unidirectional stress condition analysis, the equivalent tensile and compressive stress $\Delta\sigma_x$

applied to strip coal pillar by roof and floor strata can be calculated, and excess yield zone Δa is generated due to the tensile and compressive stress $\Delta\sigma_x$ [18,19].

$$\Delta\sigma_x = E_B\varepsilon_x, \quad \Delta a = 0.00492m\Delta\sigma_x/\gamma \tag{2}$$

where m is the thickness of coal seam; and γ is average gravity density of overlying strata.

Therefore, the equivalent tensile and compressive stress and excess yield zone of strip coal pillar for different surrounding rocks can be expressed as follows.

$$\begin{cases} \Delta\sigma_x^{'} = E_B(\varepsilon_1 - \varepsilon_3) \\ \Delta\sigma_x^{''} = E_B(\varepsilon_2 - \varepsilon_4) \\ \Delta a^{'} = 0.00492E_B(\varepsilon_1 - \varepsilon_3)/\gamma \\ \Delta a^{''} = 0.00492E_B(\varepsilon_2 - \varepsilon_4)/\gamma \end{cases} \tag{3}$$

where $\Delta\sigma_x^{'}$ is the equivalent stress of the roof and the strip coal pillar surface; $\Delta\sigma_x^{''}$ is the equivalent stress of the floor and the strip coal pillar surface; $\Delta a^{'}$ is the excess yield zone on the upper surface of the strip coal pillar; $\Delta a^{''}$ is the excess yield zone on the upper surface of the strip coal pillar; ε_1 is the strain on the lower surface of the roof; ε_2 is the strain on the upper surface of the floor; ε_3 is the strain on the upper surface of the strip coal pillar; and ε_4 is the strain on the lower surface of the strip coal pillar.

Analysis shows that, the roof and floor have a frictional effect on strip coal pillars, the lateral pressure coefficients of the interface change due to friction, and the coefficients depend on the

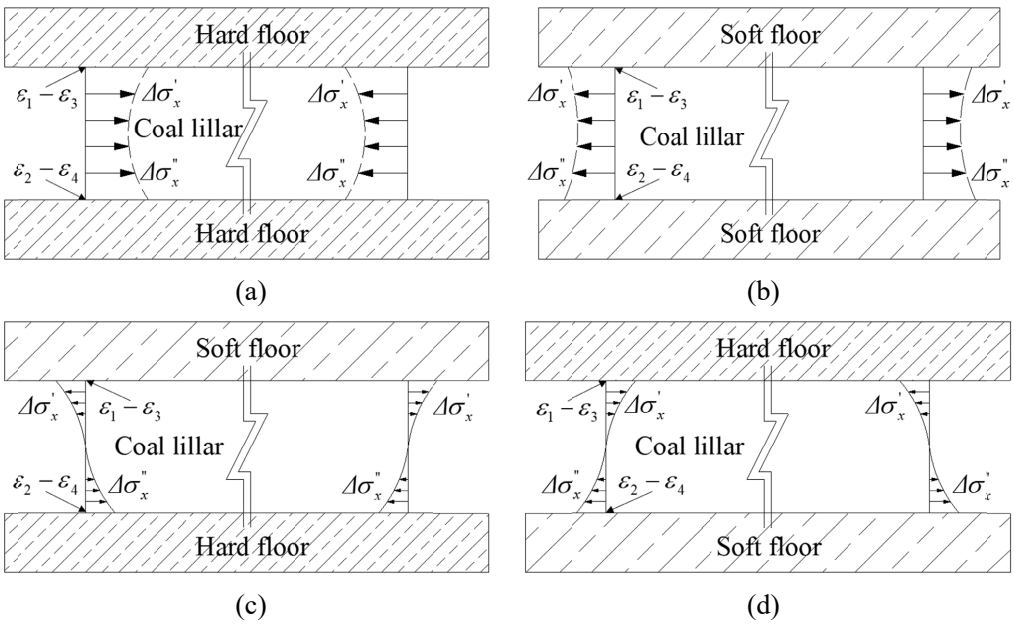

Fig. 3. Friction effect mechanical model of "roof-strip coal pillar-floor" system

elastic modulus and Poisson's ratio of the rock mass, which affects the stress state of the coal and rock mass. As shown in Fig. 3, the hard roof and floor limit the lateral displacement of strip coal pillar through friction effect, thus enhancing strip coal pillar strength and stability. In addition, the width to height ratio of strip coal pillar is large. Thus, the restraint effect spreads throughout the strip coal pillar. The interfacial cohesive force is more beneficial to the strength of strip coal pillars, which can effectively improve the stability of strip coal pillar. On the contrary, for soft surrounding rock, the friction effect is in fact causing horizontal tension in the strip coal pillar, weakening the strength of the strip coal pillar and leading to tensile failure. Therefore, for strip coal pillars in soft rock, an extra yield zone for strip coal pillars should be considered because of the tensile stress caused by the effect of friction from the roof and floor rocks.

3. Test system and preparation of the specimen

3.1. Monitoring device for strip coal pillar compression test

To study the failure characteristics and mechanisms of strip coal pillars, a monitoring device for strip coal pillar uniaxial compression testing was developed. The device consists of upper and lower pressure heads, lateral constraint pressure head, displacement sensor positioning plate, displacement sensor, data storage and processing system (Fig. 4). The pressure from the lateral constraint pressure head to the specimen is very small, the test conditions are close to uniaxial compression. Compression tests were conducted using a SHIMADIN AG-X250 electronic testing machine, in which the vertical pressure of the specimen and the lateral and vertical displacements can be monitored.

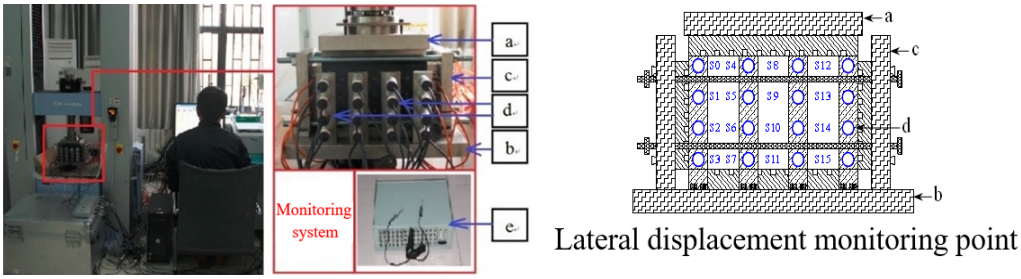

Fig. 4. Monitoring device for the strip coal pillar compression test

The monitoring device is mainly used to monitor the lateral displacement of the specimen during the test of different areas. The monitoring device consists of 8 positioning plates and 32 displacement sensors in the Y direction (Fig. 4d), and S0-S15 monitoring points are placed at the front of the specimen to monitor the lateral displacement of coal rock specimen. The displacement sensor data acquisition device is integrated into the data acquisition box (Fig. 4e). During the test, real-time data is transmitted to the acquisition system through the cable.

3.2. Monitoring device for strip coal pillar compression test

The test system includes stress loading system, failure monitoring device, and acoustic emission (AE) monitoring system (Fig. 5). The loading system uses a SHIMADIN AG-X250 electronic testing machine. The system has better stability, high precision, and can carry out uniaxial compression and tension tests with the maximum test load of 250 kN. The AE system developed by the American Physical Acoustics Corporation, which has the advantages of low noise, fast processing speed, stability, and reliability.

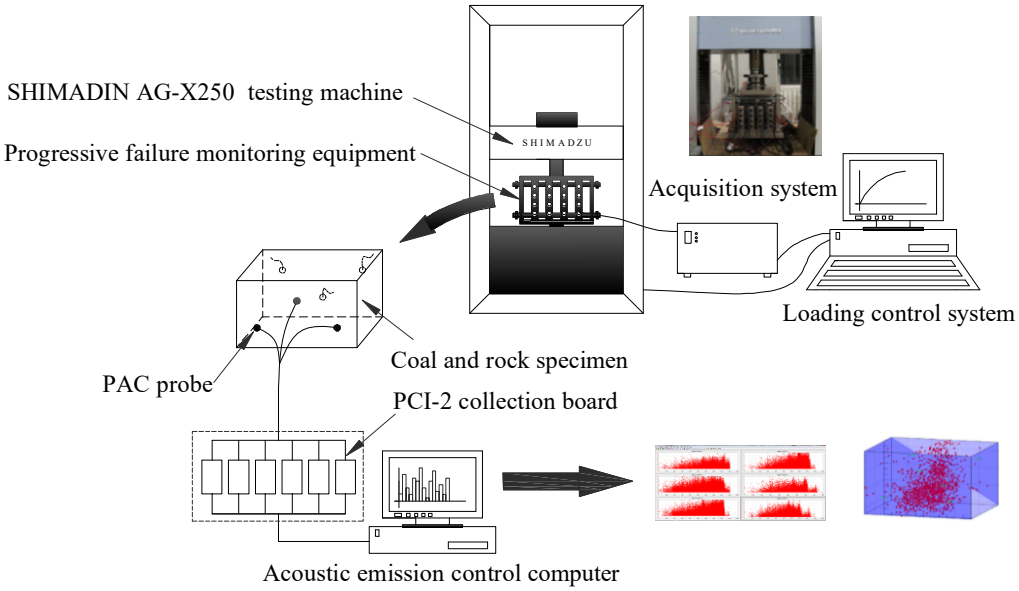

Fig. 5. Test system for the strip coal pillar uniaxial compression test

The uniaxial compression test of standard specimens was controlled by displacement, at a rate of 0.01 mm/s. Strip coal pillars are affected by surrounding rock stress and mining action for a long time, and strip coal pillars shows progressive failure characteristics. However, due to the limitations of field observations, it is difficult to observe the failure features and processes of strip coal pillars. To study the failure characteristics of strip coal pillar, a bearing test on "roof-strip coal pillar-floor" combined specimens controlled by displacement is carried out at a loading rate of 0.0002 mm/s. In addition, to enhance the coupling effect between the AE probe and specimen, Vaseline is applied to the probe and the specimen contact surface, and the probe is fixed with tape to reduce attenuation of the AE signal.

3.3. Preparation of the specimen

The mechanical properties of rock are closely related to its size. Generally, the strength and elastic modulus of a specimen gradually decrease with increasing size, and mechanical properties

tend to be more stable with increasing specimen size. A large-size specimen can more effectively simulate the mechanical characteristics of a rock-mass. However, coal is a kind of discrete and soft sedimentary rock and it is difficult to make a large complete coal specimen.

In this paper, coal samples are from the Daizhuang coal mine in Shandong province, roof and floor samples are from a medium sandstone in Daizhuang coal mine, shale in Liangjia coal mine, and red sandstone in Guangxi province. Some samples were processed into cylindrical specimen of φ50×100 mm to obtain their mechanical parameters, while others were processed into blocks 180 mm length, 60 mm wide, and 140 mm high to simulate the "roof-strip coal pillar-floor" combined specimen (Fig. 6).

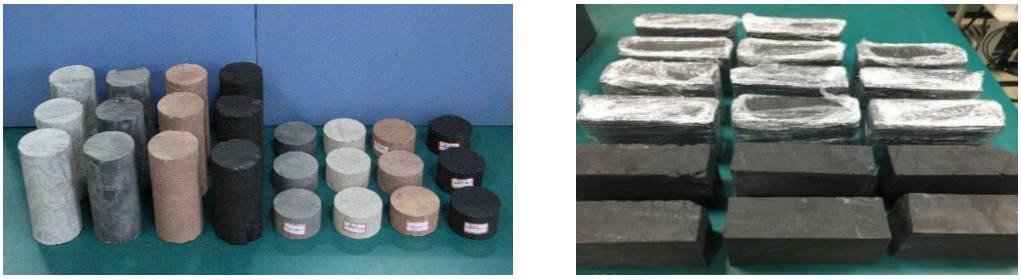

Fig. 6. Prepared coal and rock standard specimens and strip coal pillar block specimens

4. Test results

The mechanical parameters of shale, red sandstone and medium sandstone samples vary greatly (Table. 1).

TABLE 1

Mechanical parameters of coal and rock cylindrical samples

Lithology	Density g/cm^3	Ultimate strength /MPa	Tensile strength /MPa	Elastic modulus /MPa	Friction angle /°	Poisson's ratio
medium sandstone	2418.76	116.37	7.17	7563.12	39.44	0.36
red sandstone	2323.58	54.10	3.82	5908.54	37.47	0.34
shale	1981.89	42.82	4.02	2694.31	37.82	0.28
coal	1308.03	15.75	1.52	2262.43	29.98	0.26

The uniaxial compression test results of combined specimen are shown in Table. 2, with group D as control group, and the strip coal pillar without roof and floor. The uniaxial compression full stress-strain curves for the "roof-strip coal pillar-floor" combined specimen are shown in Fig. 7.

The strength of group A, group B, and group C is 13.27 MPa, 10.65 MPa, and 8.85 MPa, and the elastic modulus is 1.26 GPa, 1.12 GPa, and 0.95 GPa, respectively (Table 2). Compared with group D, the strength increased by 56.85%, 25.76%, and 4.60%, the elastic modulus of the combined specimen with medium sandstone and red sandstone increased by 28.57% and 14.28% respectively, and the elastic modulus of the shale combined specimen decreased by 3.06%. Results

TABLE 2

Uniaxial compression test results for "roof-strip coal pillar-floor" specimen

Roof and floor lithology	Number	Ultimate strength /MPa	Peak strain /×10^{-3}	Elastic modulus /MPa	Roof and floor lithology	Number	Ultimate strength /MPa	Peak strain /×10^{-3}	Elastic modulus /MPa
Medium sandstone	A-D-1	13.50	15.02	1253.02	Shale	C-D-1	8.42	15.52	851.03
	A-D-2	12.08	12.56	1208.45		C-D-2	8.82	12.23	914.55
	A-D-3	14.23	13.95	1331.78		C-D-3	9.31	15.60	1113.07
	Average value	13.27	13.84	1264.42		Average value	8.85	14.45	959.55
Red sandstone	B-D-1	10.42	13.12	1012.11	Coal	D-D-1	9.03	16.14	1055.72
	B-D-2	11.46	14.18	1266.77		D-D-2	7.89	13.84	923.84
	B-D-3	10.08	11.10	1106.46		Average Value	8.46	14.99	989.78
	Average value	10.65	12.8	1128.45					

show that uniaxial compressive strength and elastic modulus of the combined specimen increase as the roof and floor rock strength increases. This is because the hard roof and floor rock changes the lateral pressure coefficients of the coal-rock interface, the cohesive force on the interface enhances the ability to resist failure and deformation of the strip coal pillar, and the strain decreases in unit stress increment. However, the shale contains numerous bedding-parallel joints, bedding-parallel joints close gradually during compression, increasing the vertical displacement for in the same stress gradient, leading to a decreased elastic modulus, such that the peak strain is larger than that of the strip coal pillar of group D.

The stress-strain curves of the combined specimen have obvious compression, elasticity, yield, and failure stages (Fig. 7). After reaching peak strength, the specimen quickly fails, and

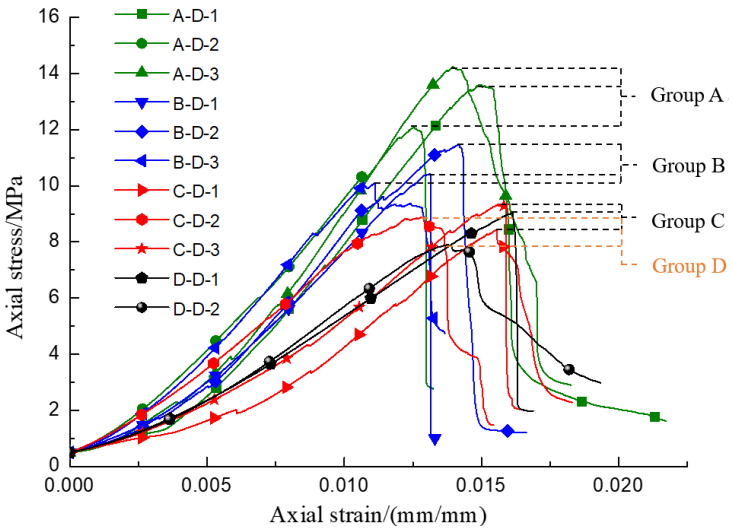

Fig. 7. Stress-strain curves of "roof-strip coal pillar-floor" specimen

the stress drops. Combined specimens have high brittleness. With increasing roof and floor rock strength, the compression stage becomes shorter, and the specimen moves directly into the elastic deformation stage. Also, the yield stage is reduced significantly. The strength of the combined specimen is higher than the group D strip coal pillar. In the combined specimen, some cracks are formed on the surface of the roof and floor rock, indicating that the roof and floor are load-bearing during the test, and the interaction between coal and rock could increase the coal pillar strength. Compared with the cylindrical standard specimens of coal, the strength of group D large-sized strip coal pillar specimens decreases, which means that the strength decreases as the specimen size increases. Also, the strength of combined specimen decreases greatly compared with the roof and floor rock. The strength of combined specimen is similar to that of group D specimens, indicating that the strength of the combined specimens is greatly influenced by the strip coal pillar.

5. Failure mechanism and characteristics of strip coal pillar

5.1. Deformation and failure process of strip coal pillar

The macroscopic deformation of coal-rock materials changes significantly before and after the destabilization and failure. The deformation values can be used to analyze the characteristics during the deformation and failure process of coal-rock materials in deep mines [20]. To study the progressive failure mechanism and characteristics of strip coal pillars, the A-D-1 as an example, and the stress and lateral displacement time curves of the specimen are plotted according to the data monitored in the test.

Unlike the standard specimen compression test, the lateral displacement of strip coal pillar increases slowly at the initial loading stage (Fig. 8). The lateral displacement appears successively when the coal pillar reaches peak strength, and lateral displacement of strip coal pillar has

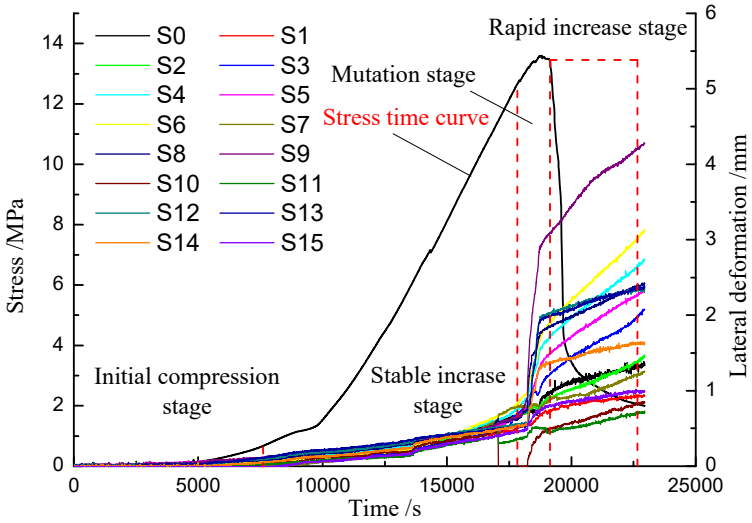

Fig. 8. Stress and lateral displacement time curves of A-D-1 specimen

obvious stages that vary with time. The failure process can be divided into four stages: initial compression stage, stable increase stage, mutation stage, and rapid increase stage. In the initial loading stage, which is the compaction of coal, rock, and the interface, the lateral displacement is small. The strength of the specimen reaches 5.37 MPa at 13500 s, vertical cracks appear at the S6 monitoring point, lateral displacement increases obviously for the first time, and the stress curve shows a drop. With continued loading, cracks gradually converge and penetrate, the volume of specimen increases, and lateral displacement increases significantly. When the specimen reaches the peak strength of 13.60 MPa at 17956 s, lateral displacement changes rapidly, and the sudden release of accumulated energy resulted in mutation of lateral displacement. Subsequently, stress rapidly drops, and the specimen enters the post peak deformation stage. The lateral displacement continues to increase, but the growth rate slows down, and the bearing capacity of the strip coal pillar decreases until overall failure of the specimen.

5.2. Progressive failure mechanism of strip coal pillar

The monitoring point when the lateral displacement reaches 0.05 mm is defined as the start of lateral displacement. The starting time and the lateral displacement maximum value curves of A-D-1 specimen are shown in Fig. 9.

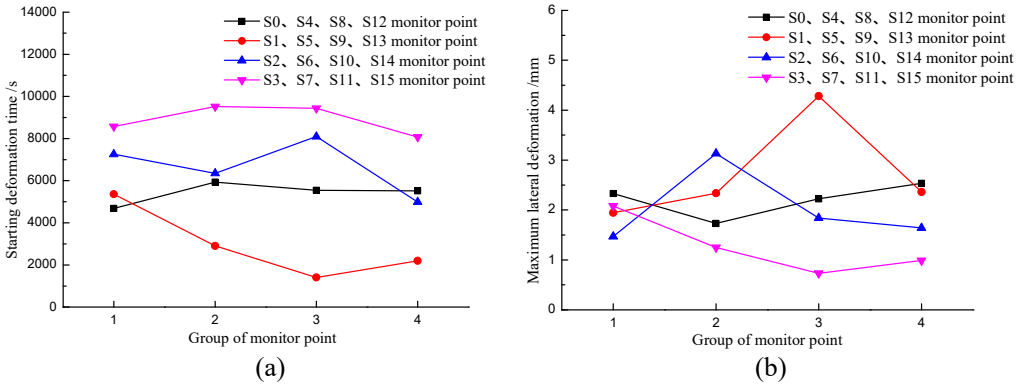

Fig. 9. The starting time and the lateral displacement maximum value curves.
(a) Starting time; (b) Lateral displacement maximum value

The lateral displacement first occurs at the S9 monitoring point in the middle of specimen at 1409 s, then S5 and S13 monitoring points showed lateral displacement at 2908 s and 2968 s respectively (Fig. 9a). With increasing load, monitor points S0 and S12 on the upper part of specimen are deformed before S4 and S8. Therefore, the middle upper position of the specimen experiences lateral displacement first, and forms the displacement change area. Stress concentrates at the corner of the specimen, then failure gradually transfers to the corner, and deformation of the lower portion of the specimen is similar to the upper portion. Lateral displacement of the S9 and S6 monitoring points are 4.28 mm and 3.13 mm, which are the maximum values of the specimen (Fig. 9b). The central part of the specimen had the maximum lateral displacement. Moreover, the displacement at the corners is greater than in the middle of the specimen, because the restrictive

effect of the device leads to the accumulation of energy at the specimen corners. The sudden release of energy caused the corner of the specimen to experience collapse and spalling.

The middle upper part of the strip coal pillar begins to deform first. Then, the damage is transferred from the central area to the corners of the strip coal pillar, with the deformation at the corners, moving gradually inward. Strip coal pillar specimens contain several longitudinal cracks, crack development causes the specimen to produce plate crack damage. When under a long-term load, the energy release of the upper part of the strip coal pillar is faster than that of the lower part, which leads to high energy accumulation in the lower part, resulting in stress unbalance between the upper and lower part of the strip coal pillar. Lateral displacement occurs first in the middle upper edge of the specimen. Moreover, the lateral displacement of the upper part of the strip coal pillar is larger than that of the lower part, and the ratio is about 2:1.

5.3. Mutation lateral displacement characteristics of strip coal pillar

Uniaxial and triaxial compression tests show that the stress-strain curves for the coal and rock specimens are smooth and continuous, and the circumferential displacement of standard cylindrical specimens increases smoothly. In this test, the size of the strip coal pillar specimen is larger, the internal cracks are well preserved, and the loading rate is small, such that subtle characters of the lateral displacement can be monitored. Lateral displacement presents step and mutation characteristics.

For the A-D-1 specimen, lateral displacement curves of S2, S6, S10, and S14 monitor points are shown in Fig. 10. The displacement curves are not smooth in comparison to past experiments but show obvious mutation characteristics. The lateral displacement of strip coal pillar has obvious mutations at 9000 s, 13800 s, and 18250 s. Displacement of the S14 monitoring point increases by 0.03 mm at 9000 s, and displacement of the S2, S6, S10, and S14 monitoring points increases by about 0.05 mm at 13800 s. As the load increases, the elastic energy in the strip coal pillar increases, and the lateral displacement mutation increment increases. Displacement of the S2, S6, S10, and S14 monitoring points increases by approximately 0.2 mm, 0.8 mm, 0.7 mm, and 1.5 mm respectively at 18250 s.

Elastic displacement occurred during loading of the specimen. In this case the axial stress applied by the loading system is converted into elastic potential energy, which is stored in the interior of the coal-mass. Slow loading can increase the dissipation of the input energy in the rock-mass, and micro defects and plastic deformation in the coal-mass units will be fully developed, resulting in an irreversible damage to the coal-mass [21]. First, a local tensile stress concentration is formed at coal-rock unit micro defects, and then extensional wing cracks are formed on the edge of the defects, which causes the development, and expansion of cracks. Lateral displacement growth rate is small at this time. With constant energy dissipation, macroscopic cracks were formed in the coal-mass [22]. Moreover, when the strain energy is released by crack extension, it is sufficient to cover the energy consumed by the new surface, macroscopic cracks propagation and pooled. The strip coal pillar develops macroscopic fractures, and the displacement in terms of mutation is observed. It is because energy accumulation causes cracks to extend, which eventually leads to a mutation displacement of the strip coal pillar.

Extensional wing crack extension is strongly influenced by the lateral pressure [23]. When the lateral confining pressure is high, crack expansion is stable and the crack stops extending

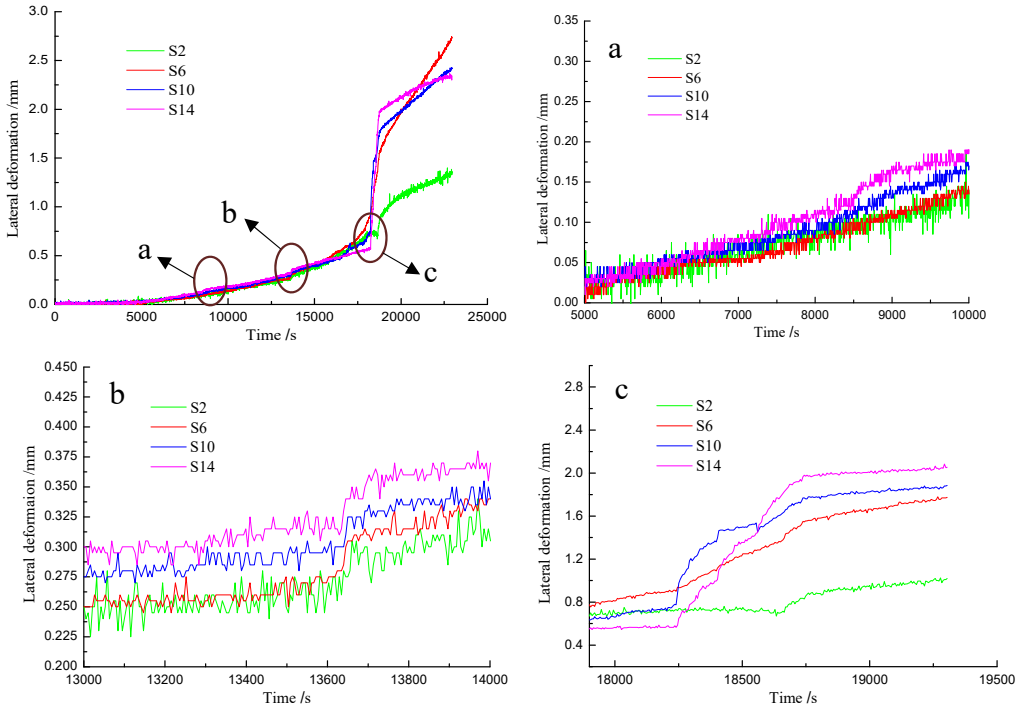

Fig. 10. Lateral displacement time curves of A-D-1 specimen

until it reaches a certain length. When the lateral confining pressure is zero or very small and the system is under axial pressure, cracks will extend in the direction of the compression. In the Y direction is unconstrained free surface. The internal confining pressure of the strip coal pillar is relatively small, so cracks will propagate in the axial direction. Finally, the direction of the stress in the strip coal pillar determines the development direction of macroscopic cracks. Macroscopic cracks appear in the vertical direction. There are numerous longitudinal cracks parallel to the X-axis in the strip coal pillar, resulting in plate structure cracks and spalling near the edge of the strip coal pillar (Fig. 11).

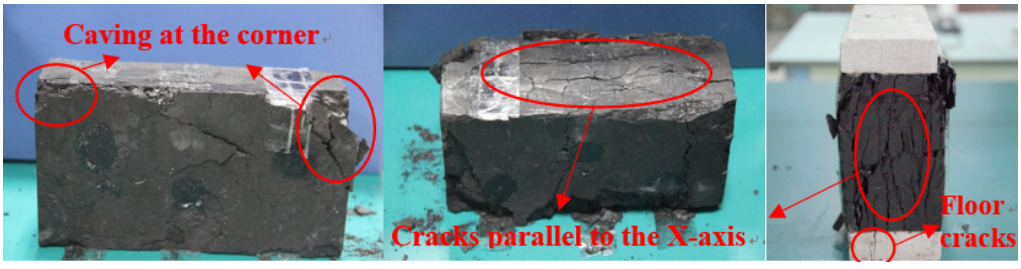

Fig. 11. Failure pictures of test specimens

6. Acoustic emission characteristics of strip coal pillar bearing tests

The closure and propagation of cracks in the coal and rock mass cause the accumulation and release of elastic energy. The AE energy rate is an important acoustic signal for characterizing the degree of energy release and failure in the coal and rock mass. The AE energy signals for specimens A-D-1, B-D-1, C-D-1, and D-D-1 are extracted for the stress time and AE energy rate time curve (Fig. 12).

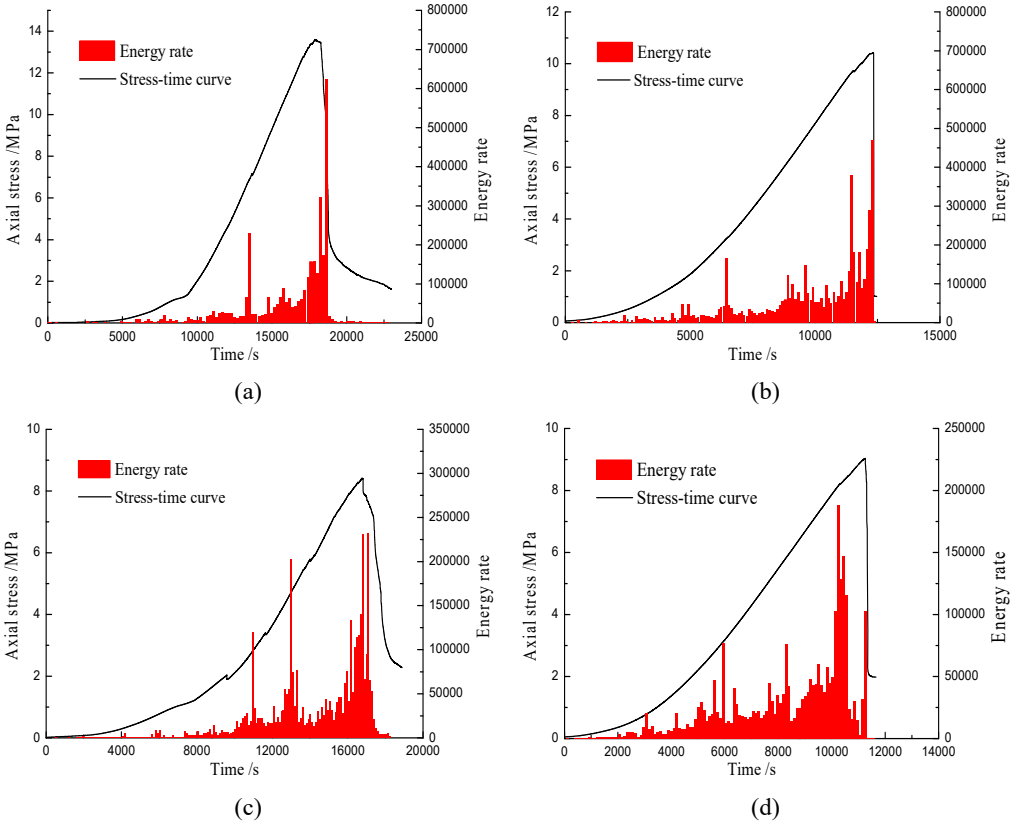

Fig. 12. Stress time and acoustic emission energy rate time curve for strip coal pillar.
(a) A-D-1; (b) B-D-1; (c) C-D-1; (d) D-D-1

The AE energy rate curve shows obvious stages. Similar to the four stages of lateral displacement in strip coal pillar, the AE signal can be divided into the initial silence stage, stable growth stage, rapid growth stage, and rapid drop stage. During early loading, damage to the rough surface and the relative slip on the original cracks produced a small amount of AE signals. With the slow increase in load, cracks propagate, new cracks appear in the coal body, energy release rate is higher, and the AE energy rate is gradually increases. With further loading, micro cracks

converge and penetrate, the AE energy rate increases in stages, and the energy rate curve shows a sudden increase-gentle-sudden increase phenomenon. As the load increases to the peak strength, many longitudinal macro cracks are formed in the coal body, the strip coal pillar is damaged as a whole, and the AE energy rate is reduced.

The stress growth rate decreases and the AE energy rate increases significantly before the peak strength, which is the rapid growth stage of AE signal (Fig. 12). The AE signal of each group show a similar pattern, but the location and duration are different. Therefore, the rapid growth AE signal period in the test can be regarded as a precursor for strip coal pillar failure. In addition, compared with the energy rate curve for specimen D-D-1, the AE signal of strip coal pillar under hard roof and floor is primarily concentrated in the rapid growth stage and unstable change stage. The harder the surrounding rock, the higher the AE signal concentration. The AE signal for specimen D-D-1 shows stable growth during the whole loading process. This is because the internal structure of the hard roof and floor is compact, and much elastic energy is accumulated in the closure of cracks during the loading process. Thus, the strip coal pillar fails when it reaches the limit strength, and macro crack expansion in the strip coal pillar causes the cracks in the roof and floor to accumulate and penetrate rapidly. The rock-mass releases a large amount of elastic energy in a short time and shows the rapid rise in AE energy rate, which also explains why coal mining under hard roof and floor conditions is more likely to produce rock burst.

7. Conclusions

(1) Considering the interfacial cohesive force between coal and rock, the frictional effect mechanical model of "roof-strip coal pillar-floor" system is established. The roof and floor have a frictional effect on the strip coal pillar. The frictional effect changes the mechanical properties of the coal mass at the coal-rock interface, and the equivalent tension and compression stress applied to the strip coal pillar restricts the instability failure. Strip coal pillar stability is higher under a hard roof and floor, while the stability is lower under a soft roof and floor.

(2) A test monitoring device for strip coal pillar compression test was developed, long-term bearing tests for strip coal pillars under different roof and floor conditions were carried out. Results show that, as the strength of the roof and floor increases, the compressive strength and elastic modulus of the combined specimen increase gradually. The large-sized combined specimen strength decreases as the specimen size increases. Combined specimen strength is greatly influenced by the strip coal pillar, and the interaction between coal and harder rock causes the specimen strength to increase.

(3) Lateral displacement of strip coal pillar can be divided into four stages: initial compression stage, stable increase stage, mutation stage, and rapid increase stage. The strip coal pillar failure process shows that middle upper part of the edge begins to deform first, then the deformation transferrers to the corner of the coal pillar. Instability in the strip coal pillar begins near the edge and moves to the interior gradually. Lateral displacement of the upper part of the strip coal pillar is larger than that of the lower part, and the lateral displacement presents step and mutation characteristics.

(4) AE signals during the strip coal pillar failure process can be divided into the initial silence stage, stable growth stage, rapid growth stage, and rapid drop stage. The stress growth rate decreases and the rapid growth of AE signal can be regarded as a precursor

to the instability of the strip coal pillar. Elastic energy accumulated in the roof and floor during the loading process is released in a short time, which explains why rock burst is more likely to occur under hard surrounding rock conditions in coal mining.

Acknowledgments

This study is financially supported by the Taishan Scholars Project, Postgraduate Research & Practice Innovation Program of Jiangsu Province (Grant No. KYCX20_0434), the Fundamental Research Funds for the Central Universities (Grant No. B200203079), National Natural Science Foundation of China (52074169, 51904167), Major basic research projects of Shandong Natural Science Foundation (ZR2018ZC0740).

References

[1] M.D.G. Salamon, Stability, instability and design of pillar workings. Int. J. Rock. Mech. Min. **7** (6), 613-631 (1970). DOI: https://doi.org/10.1016/0148-9062(70)90022-7

[2] T.P. Medhurst, E.T. Brown, A study of the mechanical behaviour of coal for pillar design. Int. J. Rock. Mech. Min. **35** (8), 1087-1105 (1998). DOI: https://doi.org/10.1016/S0148-9062(98)00168-5

[3] J.N.V.D. Merwe, Predicting coal pillar life in South Africa. J. S. Afr. I. Min. Metall. **103** (5), 293-301 (2003).

[4] A.W. Kahir, S.S. Peng, Causes and mechanisms of massive pillar failure in a southern west virginia coal mine. Int. J. Rock. Mech. Min. **22** (6), 189-189 (1985). DOI: https://doi.org/10.1016/0148-9062(85)90193-7

[5] E. Ghasemi, M. Ataei, K. Shahriar, Prediction of global stability in room and pillar coal mines. Nat. Hazards. **72** (2), 405-422 (2014). DOI: https://doi.org/10.1007/s11069-013-1014-2

[6] V. Kajzar, R. Kukutsch, P. Waclawik, J. Nemcik, Innovative approach to monitoring coal pillar deformation and roof movement using 3d laser technology. Procedia. Eng. **191**, 873-879 (2017). DOI: https://doi.org/10.1016/j.proeng.2017.05.256

[7] W.J. Guo, H.L. Wang, Z.P. Liu, Coal pillar stability and surface movement characteristics of deep wide strip pillar mining. J. Min. Saf. Eng. **32** (3), 369-375 (2015). DOI: https://doi.org/10.13545/j.cnki.jmse.2015.03.004

[8] S.J. Chen, X. Qu, D.W. Yin, X.Q. Liu, H.F. Ma, H.Y. Wang, Investigation lateral deformation and failure characteristics of strip coal pillar in deep mining. Geomech. Eng. 14 (5), 421-428 (2018). DOI: https://doi.org/10.12989/gae.2018.14.5.421

[9] S.J. Chen, D.W. Yin, N. Jiang, F. Wang, Z.H. Zhao, Mechanical properties of oil shale-coal composite samples. Int. J. Rock. Mech. Min. **123**, 104-120 (2019). DOI: https://doi.org/10.1016/j.ijrmms.2019.104120

[10] Y. Tan, W.B. Guo, Y.H. Zhao, Engineering stability and instability mechanism of strip Wongawilli coal pillar system based on catastrophic theory. J. China. Coal. Soc. **41** (7), 1667-1674 (2016). DOI: https://doi.org/10.13225/j.cnki.jccs.2015.1593

[11] J.H. Xu, X.X. Miao, X.C. Zhang, Analysis of the time-dependence of the coal pillar stability. J. China. Coal. Soc. **30** (4), 433-437 (2005).

[12] T. Sherizadeh, P.S.W. Kulatilake, Assessment of roof stability in a room and pillar coal mine in the u.s. using three-dimensional distinct element method. Tunn. Undergr. Sp. Tech. **59**, 24-37 (2016). DOI: https://doi.org/10.1016/j.tust.2016.06.005

[13] G.L. He, D.C. Li, Z.W. Zhai, G.Y. Tang, Analysis of instability of coal pillar and stiff roof system. J. China. Coal. Soc. **32** (9), 897-901 (2007). DOI: https://doi.org/10.1016/S1872-2067(07)60020-5

[14] W. Gao, M.M. Ge, Stability of a coal pillar for strip mining based on an elastic-plastic analysis. Int. J. Rock. Mech. Min. **87**, 23-28 (2016). DOI: https://doi.org/10.1016/j.ijrmms.2016.05.009

[15] J.P. Zuo, Y. Chen, F. Cui, Investigation on mechanical properties and rock burst tendency of different coal-rock combined bodies. J. China. U. Min. Techno. **47** (1), 81-87 (2018).

[16] J.P. Zuo, Y. Chen, J.W. Zhang, J.T. Wang, Y.J. Sun, G.H. Jiang, Failure behavior and strength characteristics of coal-rock combined body under different confining pressures. J. China. Coal. Soc. **41** (11), 2706-2713 (2016). DOI: https://doi.org/10.13225/j.cnki.jccs.2016.0456

[17] S.J. Chen, D.W. Yin, B.L. Zhang, H.F. Ma, X.Q. Liu, Mechanical characteristics and progressive failure mechanism of roof-coal pillar structure. Chin. J. Rock. Mech. Eng. **36** (7), 1588-1598 (2017). DOI: https://doi.org/10.13722/j.cnki.jrme.2016.1282

[18] B.N. Hu, Stability analysis of coal pillar in strip mining. J. China. Coal. Soc. **20** (2), 205-210 (1995). DOI: https://doi.org/10.13225/j.cnki.jccs.1995.02.020

[19] A.H. Wilson, An hypothesis concerning pillar stability. Min. Eng. **131** (6), 409-417 (1972).

[20] J.K. Xu, R. Zhou, D.Z. Song, N. Li, K. Zhang, D.Y. Xi, Deformation and damage dynamic characteristics of coal-rock materials in deep coal mines. Int. J. Damage. Mech. **28** (1), 58-78 (2019). DOI: https://doi.org/10.1177/1056789517741950

[21] H.P. Xie, Y. Ju, L.Y. Li, R.D. Peng, Energy mechanism of deformation and failure of rock masses. Chin. J. Rock. Mech. Eng. **27** (9), 1729-1740 (2008).

[22] Z.H. Zhao, H.P. Xie, Energy Transfer and Energy Dissipation in Rock Deformation and Fracture. J. Sichuan. Univ. **40** (2), 26-31 (2008).

[23] L.R. Myer, J.M. Kemeny, Z. Zheng, R. Suarez, R.T. Ewy, N.G.W. Cook, Extensile cracking in porous rock under differential compressive stress. Appl. Mech. Rev. **45** (8), 263-280 (1992). DOI: https://doi.org/10.1115/1.3119758